

Electron Mobility in ZnMgO/ZnO Heterostructures in the Bloch-Grüneisen Regime

To cite this article: Qun Li et al 2013 Appl. Phys. Express 6 121102

View the article online for updates and enhancements.

You may also like

- Comparative study of ZnMgO/GaAs and ZnMgO/Si solar cells Wei Zhang and Naiyun Tang
- Electron transport in ZnMgO/ZnO heterostructures Qun Li, Jingwen Zhang, Zhiyun Zhang et
- Micro-mechanism study of the effect of Cd-free buffer layers ZnXO (X = Mq/Sn) on the performance of flexible Cu₂ZnSn(S, Se), solar cell Caixia Zhang, , Yaling Li et al.



Electron Mobility in ZnMgO/ZnO Heterostructures in the Bloch-Grüneisen Regime

Qun Li¹, Jingwen Zhang^{1*}, Jing Chong², and Xun Hou¹

Received October 30, 2013; accepted November 19, 2013; published online December 4, 2013

The temperature dependence of the electron mobility in ZnMgO/ZnO heterostructures in the Bloch–Grüneisen regime is studied and many-body effects are taken into account. For sufficiently low temperatures, the mobility limited by acoustic scattering follows a stronger, $\mu \sim T^{-\alpha}$ ($\alpha = 8.5$ for the deformation-potential scattering, $\alpha = 6.5$ for the piezoelectric scattering), temperature dependence, which is significantly different from the traditional $\mu \sim T^{-1}$ law. Many-body effects play an important role in the electron transport. The theoretical calculations are able to explain recently published experimental data. © 2013 The Japan Society of Applied Physics

n the traditional theory of electron transport in the two-dimensional electron gas (2DEG), the acoustic scattering is assumed to be elastic and the phonon distribution is approximated by the equipartition law, since the phonon energy is negligibly small compared with the thermal energy of electrons (i.e., $\hbar\omega_Q\ll k_{\rm B}T$, where \hbar is the reduced Planck's constant, ω_Q is the frequency of the lattice vibration for any wave vector Q and k_B is Boltzmann's constant). However, at lower temperatures when the acoustic phonon energy is comparable to the thermal energy of electrons, the electron transport process enters the low-temperature Bloch-Grüneisen (BG) regime and the traditional theory is no longer valid. The onset temperature T_{BG} for the BG regime is given by $k_{\rm B}T_{\rm BG}=2k_{\rm F}\hbar u,^{1)}$ where $k_{\rm F}$ is the Fermi wave vector of the 2DEG and u is, depending on the phonon mode involved, the longitudinal or transverse velocity of sound. As the temperature drops below T_{BG} , acoustic phonons with wave vector $q \approx 2k_{\rm F}$ cease to be thermally excited, and only acoustic phonons with wave vector $q < 2k_F$ can interact with electrons through small-angle scattering. The phasespace restriction drastically decreases the electron-acoustic phonon interactions, and thus causes a faster increase in the 2DEG mobility like in the $\mu \sim T^{-\alpha}$ law, which is significantly different from the $\mu \sim T^{-1}$ law that follows from the traditional theory. The BG behavior of 2DEG was observed in high-purity heterostructure materials in which the extrinsic scattering mechanisms, e.g., charged impurities, interface roughness, dislocations, etc., are significantly eliminated.^{2,3)}

In this study, we develop the transport theory in ZnMgO/ZnO heterostructures in the BG regime. Many-body effects (exchange and correlation) within the local-field correction (LFC) are taken into account. The theoretical calculations are used to explain the experimental observations reported by Falson et al.³⁾

In the BG regime, we still assume that electron–acoustic phonon collisions are elastic, thus a closed-form expression for the momentum relaxation time $\tau(E)$ can be written as

$$\tau_{j}^{-1}(E) = \frac{m^{*}}{\hbar^{3}} \frac{4V}{(2\pi)^{2}} \int_{0}^{\pi} d\theta (1 - \cos\theta)$$
$$\times \int_{0}^{\infty} dq_{z} |I(q_{z})|^{2} \frac{|c_{j}(q, q_{z})|^{2}}{\epsilon^{2}(q, T)}$$

$$\times \frac{1}{1 - f_0(E)} \{ N_Q [1 - f_0(E + \hbar \omega_Q)] + (N_Q + 1)[1 - f_0(E - \hbar \omega_Q)] \}, \tag{1}$$

where m^* is the electron effective mass, θ is the angle between electron wave vectors before and after scattering, V is the sample volume, $f_0(E) = 1/\{\exp[(E - E_F)/k_B T] + 1\}$ Fermi-Dirac distribution function, $N_O =$ is $1/[\exp(\hbar\omega_Q/k_BT)-1]$ is the phonon distribution function, E is the electron energy, $E_{\rm F}$ is the Fermi level, $\hbar\omega_{O}$ is the phonon energy, q and q_z are components of 3D wave vector Q parallel and normal to the 2DEG plane, respectively, $|I(q_z)|^2 = b^6/(b^2 + q_z^2)^3$ is the overlap integral for intraband scattering, b is a variational parameter determined based on the Fang-Howard wave function,⁵⁾ $|c_j(q, q_z)|^2$ is the matrix element for the scattering mode j with $|c_1(q, q_z)|^2 =$ $D^2\hbar Q/2V\rho u_1$ for deformation-potential (DP) scattering,⁴⁾ $|c_2(q, q_z)|^2 = K^2 e^2 \hbar \omega_O / 2V \varepsilon_0 \varepsilon_s Q^2$ for piezoelectric (PE) scattering, u_1 (u_t) is the longitudinal (transverse) velocity of sound, D is the DP constant, ρ is the mass density, K^2 is the PE constant, e is the electron charge, ε_0 is the permittivity of free space, ε_s is the static permittivity, and the screening function $\epsilon(q,T)$ is given below. In contrast to the traditional theory, the complete forms of N_O and $f_0(E \pm \hbar\omega_Q)$ are retained. The screening function $\epsilon(q,T)$ used in Eq. (1) is written as

$$\epsilon(q,T) = 1 + \frac{e^2}{2\varepsilon_0 \varepsilon_s q} H(q) \Pi(q,T) [1 - G(q)], \qquad (2)$$

where $H(q)=(1+9q/8b+3q^2/8b^2)/(1+q/b)^3$ is the form factor, and $\Pi(q,T)$ is the finite temperature polarizability calculated using the Maldague formula. Many-body effects described by the LFC, including the exchange and correlation effects, are taken into account in $\epsilon(q,T)$ by introducing [1-G(q)]. We use an analytical expression for G(q), so i.e., $G(q)=1.402r_{\rm s}^{4/3}q/\sqrt{2.644}C_1^2q_{\rm s}^2+C_2^2r_{\rm s}^{4/3}q^2-C_3r_{\rm s}^{2/3}q_{\rm s}q$, where $q_{\rm s}=2/a^*$ is the screening wave number, a^* is the effective Bohr radius, $r_{\rm s}=1/\sqrt{\pi a^{*2}N_{\rm s}}$ is the Wigner–Seitz parameter, and $N_{\rm s}$ is the 2DEG density; the three coefficients C_i (i=1,2,3) are quoted from Ref. 8. For lower densities where $r_{\rm s}>1$, the LFC is important. The BG behavior of the 2DEG was observed only in high-purity heterostructure materials with densities in the vicinity of $N_{\rm s}=1\times10^{11}$ cm⁻². For $N_{\rm s}=1\times10^{11}$ cm⁻² in the ZnMgO/ZnO hetero-

¹ Key Laboratory for Physical Electronics and Devices of the Ministry of Education, Key Laboratory of Photonics Technology for Information of Shaanxi Province and ISCAS-XJTU Joint Laboratory of Functional Materials and Devices for Informatics, School of Electronics and Information Engineering, Xi'an Jiaotong University, Xi'an 710049, China

² China Satellite Maritime Tracking and Control Department, Jiangyin 214431, China E-mail: jwzhang@mail.xjtu.edu.cn

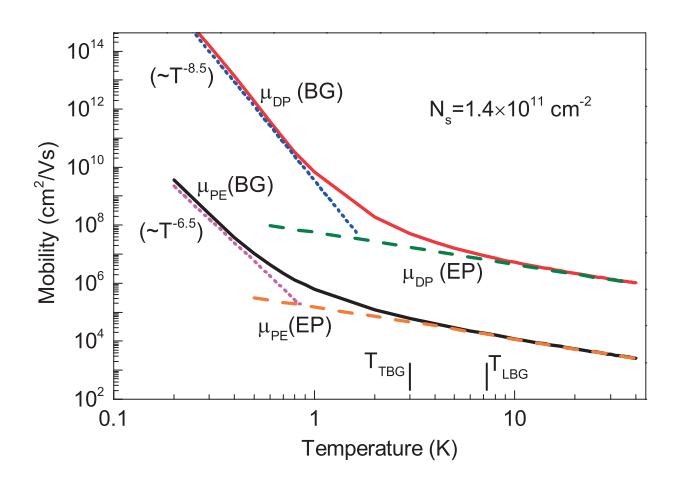


Fig. 1. Acoustic-phonon-limited mobility of the 2DEG in ZnMgO/ZnO heterostructure as a function of temperature for $N_s = 1.4 \times 10^{11}$ cm⁻². The solid lines represent the DP and PE scatterings calculated from Eq. (1), the dashed lines represent the DP and PE scatterings calculated using the traditional theory in which the equipartition (EP) law is used, and the dotted lines represent the asymptotes of the mobility in the low-temperature limit. $T_{\rm LBG} = 7.2$ K ($T_{\rm TBG} = 3.0$ K) is the onset temperature for the BG regime for longitudinal (transverse) acoustic phonon mode.

structure, $r_s = 8$, indicating that the LFC plays an important role in the BG behavior. The random-phase approximation (RPA) is given by setting G(q) = 0. For higher densities where $r_s \ll 1$, the LFC can be neglected, and accordingly, the $\epsilon(q, T)$ approaches the result within the RPA.

In the published literature concerning the electron transport in ZnO-based materials, the DP constant D is usually treated as a fitting parameter and the fitted values range from 3.8 to $15 \,\mathrm{eV}$. The difference between the fitted values of D is mainly due to imprecise measurements of the experimental data. In this study, we use $D = 3.8 \,\mathrm{eV}$ for calculations for the DP scattering. The PE constant K^2 is calculated using the piezoelectric tensor components $h_{15} = -0.37$, $h_{31} = -0.62$, and $h_{33} = 0.96 \,\mathrm{C/m^2}$. $h_{31}^{13,14}$.

Figure 1 shows the calculated mobility limited by acoustic DP and PE scatterings as a function of temperature. At higher temperatures, the mobility calculated from Eq. (1) is proportional to T^{-1} , which is consistent in the result that follows from the traditional theory. This is because the simplified approximations, $N_Q \approx k_{\rm B}T/\hbar\omega_Q$ and $f_0(E \pm \hbar\omega_Q) \approx f_0(E)$, used in the traditional theory are valid at higher temperatures. As the temperature drops below the onset temperature $T_{\rm BG}$ for the BG regime, the temperature dependence of the mobility undergoes a smooth transition from the $\mu \sim T^{-1}$ law to the $\mu \sim T^{-\alpha}$ law; $\alpha = 8.5$ ($\alpha = 6.5$) for the DP (PE) scattering. According to $k_B T_{BG} = 2k_F \hbar u$ and $u_1 > u_t$, the onset temperature T_{BG} for the longitudinal acoustic phonon mode is larger than that for the transverse acoustic phonon mode, i.e., $T_{LBG} > T_{TBG}$. The DP-limited mobility $\mu_{DP}(BG)$ is dominated by the longitudinal acoustic phonon mode; accordingly, $\mu_{\mathrm{DP}}(\mathrm{BG})$ deviates from $\mu_{\mathrm{DP}}(\mathrm{EP})$ (mobility calculated using the traditional theory) below T_{LBG} . In contrast, the PE-limited mobility $\mu_{PE}(BG)$ is dominated by the transverse acoustic phonon mode; accordingly, $\mu_{PE}(BG)$ deviates from $\mu_{PE}(EP)$ below T_{TBG} .

Figure 2 shows the importance of many-body effects described by the LFC for the 2DEG mobility. The mobility calculated using the LFC shows a temperature dependence

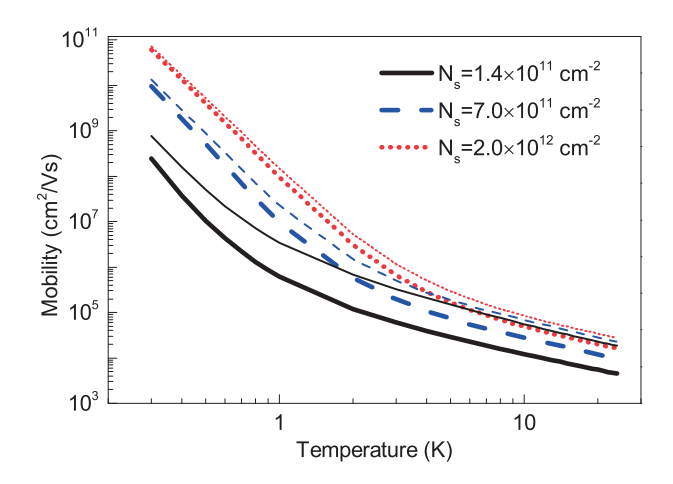
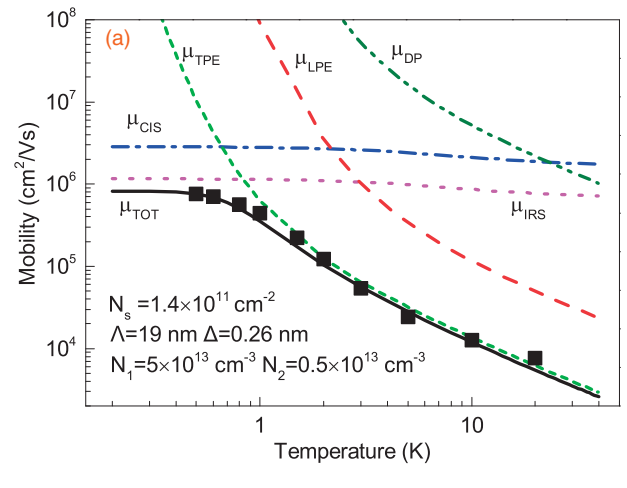


Fig. 2. Acoustic-phonon-limited mobility of the 2DEG in ZnMgO/ZnO heterostructure as a function of temperature for different 2DEG densities. The thick lines indicate the data calculated using the LFC and the thin lines indicate those calculated using the RPA.

similar to that calculated using the RPA. However, many-body effects greatly decrease the screening effects of the 2DEG, leading to a decrease in the mobility, particularly for lower densities. As the 2DEG density increases, many-body effects become relatively less important. However, the influence of many-body effects is still large for $N_{\rm s} = 2.0 \times 10^{12} \, {\rm cm}^{-2}$.

Recently, Falson et al.³⁾ observed a strong temperature dependence of the 2DEG mobility in ZnMgO/ZnO heterostructures at lower temperatures. It can be seen in Fig. 3 that as the temperature decreases below 10 K, the temperature dependences of the mobilities for $N_s = 1.4 \times 10^{11}$ and 6.8×10^{11} $10^{10}\,\mathrm{cm^{-2}}$ are stronger than the high-temperature $\mu \sim T^{-1}$ dependence, exhibiting obvious characteristics of the BG behavior, and the mobilities start saturating below 1 K. We attempt to explain the experimental observations using our transport theory for the BG regime. The charged impurity scattering (CIS) and the interface roughness scattering (IRS) are viewed as two important extrinsic scattering mechanisms limiting the low-temperature saturation mobility of the 2DEG in ZnMgO/ZnO heterostructures. 15) In the fittings to the experimental data, therefore, the CIS and IRS are taken into account using the expressions in Refs. 16 and 17, respectively, and the screening function within the LFC [as shown in Eq. (2)] is taken into account. It is assumed that the impurities are evenly distributed in ZnMgO at a density of N_1 , and in ZnO at a density of N_2 . Optical phonon scattering is ignored in the fittings since this scattering mechanism is important only at temperatures above 100 K.¹⁸⁾ In the fittings, only the parameter values associated with the extrinsic scattering mechanisms, i.e., the impurity densities N_1 in ZnMgO and N_2 in ZnO, the height Δ and lateral size Λ of roughness, are adjustable.

The temperature dependence of the mobility limited by individual scattering mechanisms for $N_{\rm s}=1.4\times10^{11}\,{\rm cm^{-2}}$ is shown in Fig. 3(a). It is found that the IRS dominates the saturation mobility at low temperature. The temperature-dependent behavior of the mobility is dominated by the transverse-PE scattering. The weak temperature-dependences of $\mu_{\rm CIS}$ and $\mu_{\rm IRS}$ are due to the temperature-dependent screening effects as shown in Eq. (2). In Fig. 3(b), the experimental results for another four samples with different 2DEG densities are fitted by calculations. It can be seen



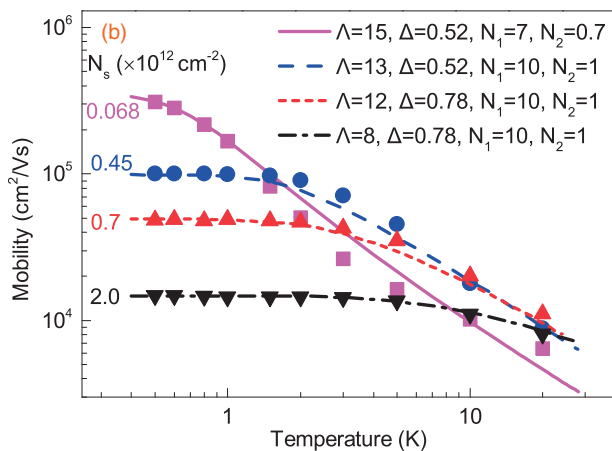


Fig. 3. Temperature dependence of calculated mobility limited by (a) individual scattering mechanisms, including DP scattering (μ_{DP}), longitudinal-PE scattering (μ_{LPE}), transverse-PE scattering (μ_{TPE}), charged impurity scattering (μ_{CIS}), interface roughness scattering (μ_{IRS}), and all scattering mechanisms (μ_{TOT}) mentioned above, for $N_s=1.4\times10^{11}\,\mathrm{cm}^{-2}$ and (b) all scattering mechanisms for $N_s=6.8\times10^{10}$, 4.5×10^{11} , 7.0×10^{11} , and $2.0\times10^{12}\,\mathrm{cm}^{-2}$. The scattered symbols are the experimental data from Ref. 3. The unit of Λ and Δ is nm; the unit of N_1 and N_2 is $\times10^{13}\,\mathrm{cm}^{-3}$.

in Fig. 3 that all the experimental data can be explained satisfactorily using our theory without adjusting the parameter values of D and K^2 .

In conclusion, we studied the temperature dependence of the 2DEG mobility in ZnMgO/ZnO heterostructures in the BG regime. In the low-temperature limit, the mobility is proportional to $T^{-8.5}$ ($T^{-6.5}$) for the DP (PE) scattering. Manybody effects effectively decrease the 2DEG mobility, particularly for lower densities. The theoretical calculations are in good agreement with recently published experimental data.

Acknowledgments This work was supported by the National Natural Science Foundation of China under Grant Nos. 61176018 and 60876042, and the National High Technology Research and Development Program of China (863 Program) under Grant No. SQ2013GX04D00825.

- 1) P. J. Price: Solid State Commun. 51 (1984) 607.
- H. L. Stormer, L. N. Pfeiffer, K. W. Baldwin, and K. W. West: Phys. Rev. B 41 (1990) 1278.
- J. Falson, D. Maryenko, Y. Kozuka, A. Tsukazaki, and M. Kawasaki: Appl. Phys. Express 4 (2011) 091101.
- 4) T. Kawamura and S. D. Sarma: Phys. Rev. B 45 (1992) 3612.
- 5) F. F. Fang and W. E. Howard: Phys. Rev. Lett. 16 (1966) 797.
- 6) P. K. Basu and B. R. Nag: J. Phys. C 14 (1981) 1519.
- 7) P. F. Maldague: Surf. Sci. 73 (1978) 296.
- 8) A. Gold: Z. Phys. B 103 (1997) 491.
- 9) A. Gold: J. Appl. Phys. 110 (2011) 043702.
- D. L. Rode: Semiconductors and Semimetals: Low-Field Electron Transport (Academic, New York, 1975) p. 84.
- F. Bertazzi, E. Bellotti, E. Furno, and M. Goano: J. Electron. Mater. 38 (2009) 1677.
- 12) D. C. Look, D. C. Reynolds, J. R. Sizelove, R. L. Jones, C. W. Litton, G. Cantwell, and W. C. Harsch: Solid State Commun. 105 (1998) 399.
- 13) I. B. Kobiakov: Solid State Commun. 35 (1980) 305.
- 14) S. B. Lisesivdin, A. Yildiz, N. Balkan, M. Kasap, S. Ozcelik, and E. Ozbay: J. Appl. Phys. 108 (2010) 013712.
- 15) S. Akasaka, A. Tsukazaki, K. Nakahara, A. Ohtomo, and M. Kawasaki: Jpn. J. Appl. Phys. 50 (2011) 080215.
- 16) M. N. Gurusinghe, S. K. Davidsson, and T. G. Andersson: Phys. Rev. B 72 (2005) 045316.
- 17) B. K. Ridley, B. E. Foutz, and L. F. Eastman: Phys. Rev. B 61 (2000) 16862.
- 18) W. Walukiewicz, H. E. Ruda, J. Lagowski, and H. C. Gatos: Phys. Rev. B 30 (1984) 4571.